

RADIATION SHIELDING ASPECTS FOR LONG MANNED MISSION TO SPACE – Criteria, Survey Study, and Preliminary Model –

by

**Manuel SZTEJNBERG, Shanjie XIAO, Nader SATVAT,
Felisa LIMÓN, John HOPKINS and Tatjana JEVREMOVIC**

Received on November 14, 2006; accepted in revised form on December 3, 2006

The prospect of manned space missions outside Earth's orbit is limited by the travel time and shielding against cosmic radiation. The chemical rockets currently used in the space program have no hope of propelling a manned vehicle to a far away location such as Mars due to the enormous mass of fuel that would be required. The specific energy available from nuclear fuel is a factor of 10^6 higher than chemical fuel; it is therefore obvious that nuclear power production in space is a must. On the other hand, recent considerations to send a man to the Moon for a long stay would require a stable, secured, and safe source of energy (there is hardly anything beyond nuclear power that would provide a useful and reliably safe sustainable supply of energy). National Aeronautics and Space Administration (NASA) anticipates that the mass of a shielding material required for long travel to Mars is the next major design driver. In 2006 NASA identified a need to assess and evaluate potential gaps in existing knowledge and understanding of the level and types of radiation critical to astronauts' health during the long travel to Mars and to start a comprehensive study related to the shielding design of a spacecraft finding the conditions for the mitigation of radiation components contributing to the doses beyond accepted limits. In order to reduce the overall space craft mass, NASA is looking for the novel, multi-purpose and multi-functional materials that will provide effective shielding of the crew and electronics on board. The Laboratory for Neutronics and Geometry Computation in the School of Nuclear Engineering at Purdue University led by Prof. Tatjana Jevremovic began in 2004 the analytical evaluations of different lightweight materials. The preliminary results of the design survey study are presented in this paper.

Key words: long mission to space, cosmic radiation, shielding, Monte Carlo method, radiation transport

INTRODUCTION

Increased understanding of space radiation environment, development of novel materials with better performance in various radiation fields, as well as an exponential development of computer hardware and improvements in computational

models allow for advances in designing the radiation shielding meeting dose limits for humans and equipment devices during space travel. However, there is no actual knowledge, evidence or the experimental verification of the designs for complex missions such as a manned mission to Mars, or a long stay at the Moon. The state-of-the-art approach to missions to space was based on designing the craft and the whole mission *without* taking into account the effect of space radiation. The need for possible design modifications would often be inspected after the design of the craft has been completed. The design would be modified to meet the needs if identified [1]. Possible modifications would include the improvement of essential radiation hardness of critical locations on board by choosing more effective materials, changing the mission profile, or adding

Scientific paper
UDC: 629.785:539.12
BIBLID: 1451-3994, 21 (2006), 2, pp. 47-66

Authors' address:
School of Nuclear Engineering, Purdue University
West Lafayette, IN 47907, USA

E-mail address of corresponding author:
tatjanaj@ecn.purdue.edu (T. Jevremovic)

more materials to improve the shielding against outboard radiation. However, a manned long term mission to deep space must include in the spacecraft design the radiation shielding criteria from the very beginning. Since it is impossible to expose the true space craft to a true cosmic radiation field and test the material performance in order to convert to the acceptable shielding design, the analysis and design of the space radiation shielding of the space craft rely on theoretical modeling and computational simulations. It is also becoming clearer that materials only will most likely not be enough to protect against cosmic radiation. Analysis point toward more complex craft designs including radiation repellent devices. One of such approaches is under development in the Laboratory for Neutronics and Geometry Computation (NEGE) at Purdue University and is focused at finding the way to encapsulate a spacecraft against radiation using a magnetic field generated at the front end of the craft.

The purpose of our current preliminary survey study was to develop an overall comprehensive material type & weight design area for the spacecraft shielding assuming manned mission to deep space (beyond the Earth's Moon). The material type & weight design area is defined as the range of parameters that would satisfy the criteria imposed to the spacecraft design, allowed radiation dose limits and spacecraft weight. The Monte Carlo computer codes such as COG, MCNP5, and MCNPX, [2, 3] are used to develop this survey study related to the impact of space radiation environment on the need for shielding and protection of the crew and electronic devices on board. The objective of this survey study is to avoid exceeding the allowed levels of radiation exposures and dose rates during the mission. The survey study covers:

- (a) identifying the prevailing types and sources of penetrating radiation affecting the spacecraft and mission to deep space (beyond the Earth's Moon), and selecting the space radiation-mix field (fluence and energy),
- (b) criteria for the space shielding design,
- (c) analysis and calculation of the necessary thickness of the most effective materials to attenuate each individual type of radiation in space (using two-dimensional Monte Carlo analysis of the shielding performance of selected materials) and determine the mass penalty; combination of the identified materials into a thin shielding wall and analysis of the effect of the mixed radiation field and mass penalty,
- (d) three-dimensional modeling of the space craft with occupants using the shielding design from the two-dimensional studies, and
- (e) analysis of the radiation dose limits in the spacecraft and discussion on a set of recommendations needed for future analysis and experimental studies.

PREVAILING TYPES AND SOURCES OF PENETRATING RADIATION AFFECTING THE SPACECRAFT AND MANNED MISSION TO DEEP SPACE

Primary radiation. The definition of the space radiation environment introduces by far the greatest overall uncertainty in the radiation dose prediction for manned mission to deep space. The major radiation sources of interest to deep space travel are galactic cosmic radiation (GCR) and solar energetic particles (SEPs). GCR comes from the outside of our solar system and provides a continuous, isotropic radiation source. The GCR contains approximately 85% protons, 14% alphas [4, 5] (or 90% protons, 10% alphas [5, 6]), less than 1% heavy nuclei, and negligible amount of electrons and positrons. Table 1 shows the GCR abundances of nuclei heavier than proton. Helium, carbon, and oxygen display noticeable abundances. Elements that precede nickel are often ignored in human space flight analysis because of their low abundances [8]. The energies of GCR particles vary from a few MeV per nucleon to 10^{15} MeV per nucleon; they span over fourteen orders of magnitude¹. Figure 1 shows the

Table 1. Relative GCR elemental abundances (normalized 0-1000) for $Z>1$ and $E>450$ MeV [12]

Element	Abundance
He	44700
C	1130
O	1000
B	329
N	278
Mg	203
Li	192
Ne	158
Si	141
Fe	103
Be	94
Al	36
Si	34
Na	29
Ca	26
P	24
Cr	15
Ar	14
Ti	14
Mn	12
K	10
V	9.5
Cl	9
P	7.5
Se	6
Ni	6

¹ Flux of cosmic rays on the Earth's surface is falling approximately as the inverse-cube of their energy

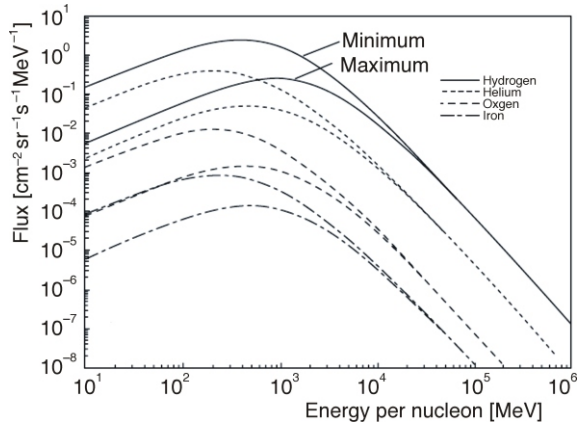


Figure 1. Differential energy spectra of GCR at solar minimum and maximum [10]

differential energy spectra for H, He, O, and Fe. It also depicts the fluctuation of GCR dependent on the 10-12 year solar cycle. During the solar minimum, an interplanetary magnetic field is the weakest, which allows more intergalactic particles to access our solar system; therefore the GCR has its largest intensity. The resulting doses from the minimum and maximum solar cycle differ by a factor of two. The change occurs mainly in the energy range between 1 and 1000 MeV. GCR also fluctuates from one solar cycle to another, showing different ranges for the peak energies. Current models [9, 10, 11] can represent history measurements within about 15% accuracy. Because of the unpredictable nature of the GCR sources, usually an average energy is selected in order to assess the risks for manned missions in deep space.

Solar energetic particle events (SEPEs) originate from coronial mass ejections in the sun that happen unpredictably throughout the solar cycle, usually around the solar maximum. SEPEs contain large fluxes of protons and heavy ions, the sources of potentially lethal radiation dose rates in a few to sev-

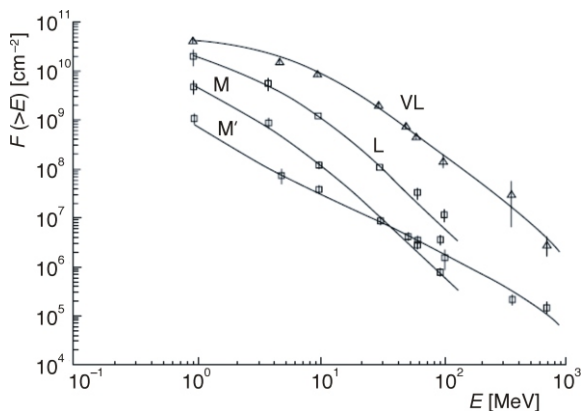


Figure 2. Integral energy spectra [10]

eral hours. Figure 2 shows the integral energy spectra (fluxes with the energy greater than a given energy, *i. e.* $F(>E)$) of averaged event fluxes at four such large events. The VL, L, M/M, means very large, large, and medium events according to Nymmik's classification [10]. The largest event recorded in recent history occurred in February of 1956 when secondary neutron levels were recorded to have increased by more than 4000%. Because of the unpredictable nature of SPEs, shielding design will have to take into account a forecasted worst case scenario in order to suitably protect the astronauts.

Table 2 summarizes the flux levels of most important external primary radiation sources found in deep space of interest to shielding survey study presented in this paper. It can be observed that the deep space radiation is mainly composed of protons. The energy of protons varies from 1 keV to several of GeV. The low energy protons from the solar wind are negligible, and the energy of protons from the GCR (as shown in fig. 1) mainly extends from 10 MeV to hundreds of GeV. On the other side, the amount of alphas present in space cannot be omitted, because they can interact with craft materials and produce a noticeable number of secondary radiation. Similarly, very high energy alpha particles are omitted due to their very small level of fluxes. The spectra of alphas can also be seen in fig. 1. Though heavy particles are important as primary radiation as well as sources of secondary radiation, they are not included in this survey study due to their small flux levels and the limitation of available numeric simulation tools and lack of the cross-section data.

Table 2. External primary radiation sources [5, 8, 10]

Radiation source	Type of radiation	Energy	Flux [$\text{cm}^{-2} \text{s}^{-1}$]
Solar wind	Protons (95%)	1 keV	$2 \cdot 10^8$ at 1 AU*
Galactic cosmic rays	Protons (90%) Alpha (10%)	10 MeV- 10^{10} GeV	2
Solar energetic particle events	Vary between events	Vary between events	Accurate prediction can not be made

* Astronomical unit

Secondary radiation. The high energy primary radiation source is expected to be a source of relatively large amount of secondary radiation produced by primary radiation interactions with the craft and shielding materials. Neutrons are the most important component of the secondary radiation for space voyage because of their high penetrability.

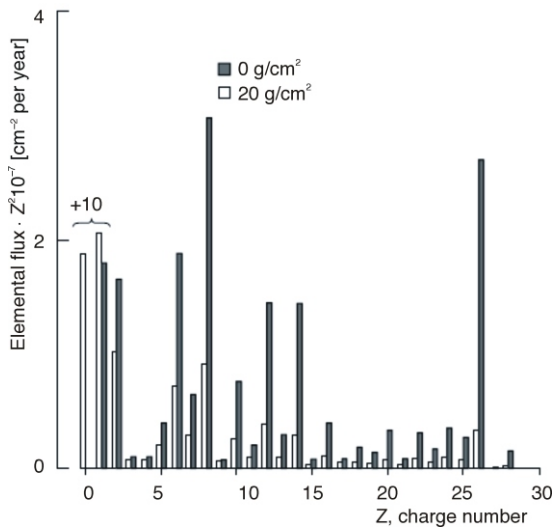


Figure 3. Calculations of elemental fluxes at 0 and 20 g/cm² of aluminum [13]

Though free neutrons do not exist in the primary radiation due to their short lifetimes, a noticeable amount of neutrons is generated through various interactions of the primary particles in shielding materials. These interactions span the full range of ions (protons, helium, and high Z elements – HZE) and energies (100 MeV per nucleon or higher). As an example, fig. 3 shows the calculated flux before and after 20 g/cm² of aluminum shielding [12]. It illustrates that though there is no neutron in the primary source, a large amount of neutrons are generated (note that the neutron flux is divided by 10). Although the relative amounts of helium and other HZE are low, their yields of secondary neutrons are high. One example shows that behind 50 g/cm² of water, about 15% of neutrons come from the helium interactions, and another 16% from the HZE interactions. Therefore, the main sources of space radiation as indicated in tab. 2 that are of concern for the spacecraft shielding design are:

- protons and electrons trapped in the Van Allen belts (not analyzed in this study),
- heavy ions trapped in the magnetosphere,
- cosmic ray protons and heavy ions (including alphas),
- protons and heavy ions from solar flares, and
- secondary radiation produced in spacecraft (neutrons, protons, electrons, X and rays).

Space radiation design criteria

Shielding materials. Space travel in the past was limited to low Earth orbits (LEO) and geosynchronous Earth orbits (GEO) holding down the knowledge of necessary shielding for space missions. Both orbits, LEO and GEO, are within the

Earth's magnetosphere and therefore, are protected from a majority of GCRs. However, for a long manned mission to space the shielding criteria must be altered to protect the astronauts in a much harsher environment. For extended spaceflight and for interplanetary missions, there is an increasing importance on the type of shielding used and its ability to attenuate primary and prevent the formation of secondary radiation; some materials block a large amount of GCRs but the secondary particles they produce counteract this effect and are more harmful to the internal environment. For example, electrons produce penetrating X-radiation, or *bremstrahlung*, as they scatter and slow on atomic nuclei. Cascades of secondary particles, similar to those produced in the atmosphere, are also produced in spacecraft and can become very significant for heavy structures. Therefore, it is not possible to use just one material to effectively shield astronauts from radiation in space; the shielding is thus expected to be complex involving a combination of different materials.

The penetrating energetic radiation in space generally has the adverse effect on the spacecraft materials, components, and occupants. The unfavorable effects refer to the changes in properties of the materials or components that impair their functionality, or physiological effects on occupants of the craft that would compromise their well-being or affect their functioning. Without providing satisfactory shielding of the craft, the space radiation may affect the whole mission resulting in its failure or permanent injury of the craft, its occupants or elements vital for safe and secured travel.

Light weight shielding materials. Several different materials are considered to replace or aid aluminum in shielding capabilities such as: liquid hydrogen, liquid methane, metallic hydrides (such as LiH_{0.98}, YH_{1.8}, ZrH_{1.33}, TiH_{1.7}), polyethylene (PE) and water. In the past, structural and electronic components of the spacecraft were utilized in order to provide additional shielding. The materials that are best as shielding even for HZE particles are those with low atomic mass and high amount of hydrogen. The polymers high in hydrogen content are more efficient than aluminum. Also using food, water and necessary components for the spacecraft would provide an additional shielding. The PE is ideal because of its lightweight and its richness in hydrogen [4].

Radiobiological effects. One of the limiting factors for deep space travel is the exposure to possibly high levels of radiation and the biological effects on the astronauts. Some assumptions can and have been made and dose estimates can be calculated based on experimental data and data received from NASA deep space probes and Mars rover missions. For long-duration interplanetary missions, most of the

radiation dose will arise from cosmic rays, solar particle ions and secondary particles. Radiation particles which are harmful to humans fall mostly in the energy range from 15 to 500 MeV because they possess enough energy to damage the DNA. Particles with energies above 500 MeV per nucleon pass through the human body so quickly that there is not enough time to transfer the energy to the tissue, [5]. Extended duration missions to Mars will pose an elevated risk of radiation exposure due to the complex nature of cosmic radiation. Radiation protection is the limiting factor to the duration of manned missions. No limits have yet been set for deep space missions; the dose limit for the International Space Station (ISS) are set at 200 mSv per year. Novel and sensible shielding must be therefore constructed to safely shield humans from the complex cosmic radiation field. Because the radiation field in deep space contains almost all types of radiation, the composition of different materials may allow for an effective solution for the shielding during deep space missions. Eventually the shield will have to pass reviews of cost, weight and production feasibility.

Most effective materials to attenuate each individual type of radiation in space

Space radiation shielding is focused at the design, fabrication, testing, and insertion of multi-functional materials that can serve as structural materials of space vehicles and habitats while providing necessary radiation shielding for the crew and systems. The design of radiation shields used to attenuate radiation from any radioactive source depends upon the location, intensity, energy distribution of the sources, and permissible radiation levels at positions away from these sources. Different materials exhibit different abilities to shield against different radiation types.

This section summarizes the computational survey study developed to evaluate the various materials that would provide best attenuation with the smallest mass penalty to the overall weight of the space craft. The study includes a brief theoretical analysis proceeded with the design area obtained from two-dimensional computational analysis based on COG, MCNP5 and/or MCNPX Monte Carlo codes [2, 3]. The computational model consists of an infinite slab exposed to a planar monoenergetic source of individual radiation types (fig. 4). In order to obtain the equivalent dose, the quality factors of 1, 1, 10, 10, and 20 were used for photons, electrons, neutrons (conservative value), protons and alphas, respectively [6]. In addition, the weight of some of the shielding materials is estimated assuming the size of the space craft room to be 5 × 5 × 3 m (according to the discussions having taken place with NASA representative in April 2006).

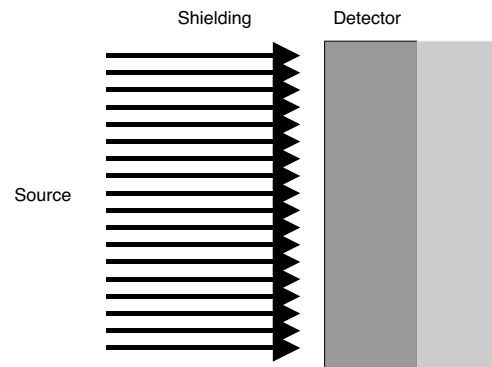


Figure 4. Two-dimensional computational shielding model¹ (COG, MCNP5, MCNPX codes)

High energy protons

Theoretical consideration. The most effective materials to shield against protons are listed in tab. 3. Taking the density into consideration, only polyethylene (PE), aluminum, iron, and hydrogen are potential candidates for the shielding design. The other materials of interest (to attenuate high energy alpha, HZE or neutrons) are various types of PE (PE with boron or lithium), and nano-carbon fibers.

Table 3. Materials effective to shield against the energetic protons

Material	Z	Density [gcm ⁻²]
Lead	82	11.37
Graphite	12	1.70
Iron	26	7.90
Tin	50	7.30
Tungsten	74	19.35
Polyethylene	–	0.95
Hydrogen	1	0.07
Aluminum	13	2.71
Paraffin wax	–	0.93
Mylar	–	1.40

Figure 5 shows a linear proton range for various materials as a function of incoming proton energy. It can be seen that lead, polyethylene and iron all demonstrate similar shielding efficiency at energies between 100 and 200 MeV. The shortest distances that the proton can travel are observed to take place in lead and iron, with ranges of 1 to 40 cm. PE

¹The shield is placed 8 cm away from the planar source and detector is placed after the shielding material

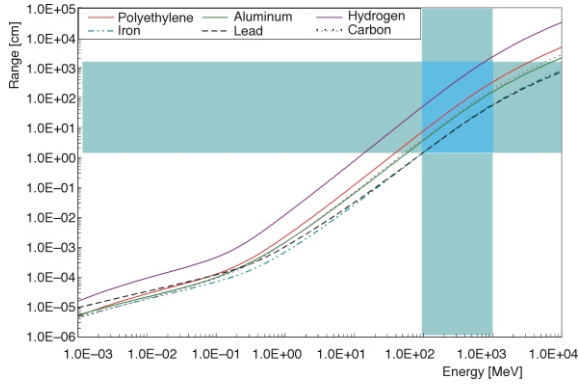


Figure 5. Linear CSDA range¹ of protons vs. energy for PE, H, Pb, Al, and Fe [19]

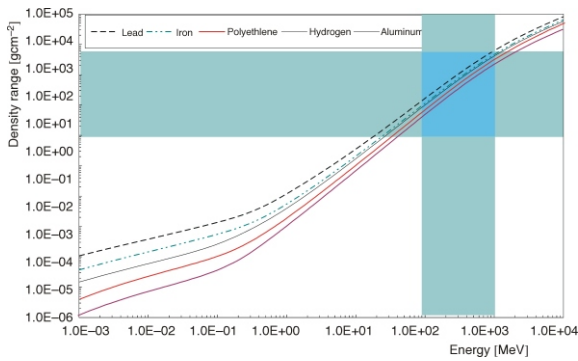


Figure 6. Density range of protons vs. energy for PE, H, Pb, Al, and Fe [19]

is the next most effective shielding material, with proton ranges from 5 cm up to 100 cm in the analyzed energy region. The density effectiveness is depicted in fig. 6. Not only do iron and lead prove to be the least efficient at shielding with concern to weight, but higher Z materials can also increase the dose because of the secondary radiation.

Figure 7 shows the design area for the spacecraft room shielding against protons, *i. e.* the shielding weight based on the range indicated in fig. 6 as a function of energy. It can be seen that PE demonstrates the anticipated performance, maintaining a

¹ CSDA range: a very close approximation to the average path length traveled by a charged particle as it slows down to rest, calculated in the continuous-slowing-down approximation. In this approximation, the rate of energy loss at every point along the track is assumed to be equal to the same as the total stopping power. Energy-loss fluctuations are neglected. The CSDA range is obtained by integrating the reciprocal of the total stopping power with respect to energy. It is higher than the Projected range in the analyzed cases.
 Projected range: average value of the depth to which a charged particle will penetrate in the course of slowing down to rest. This depth is measured along the initial direction of the particle

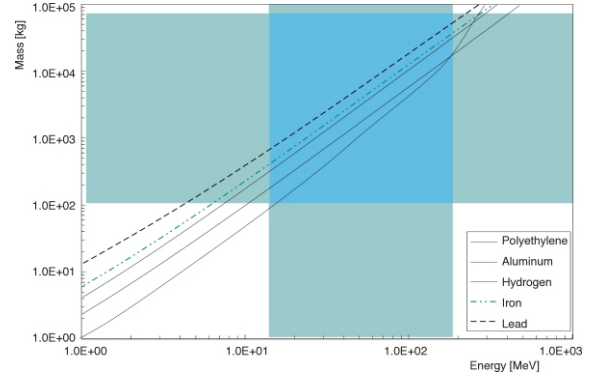


Figure 7. Weight of shielding for a room of 5 x 5 x 3 m and a thickness of CSDA range as function of particle energy and material type [19]

small weight while effectively stopping the protons of expected energies.

Numerical analysis. For the proton energy of 100 MeV and the geometry shown in fig. 4, the proton attenuation including formation of secondary radiation is analyzed for various types of PE (densities are shown in tab. 11), aluminum and nano-carbon fibers (CnM), fig. 8 and tab. 4. The production of secondary radiation varies with the atomic density of the shielding material. If hydrogen (H) is used to shield against protons, no secondary radiation is produced, while with increased Z more secondary radiation is created. A material with high H content is ideal for shielding against protons, which would reduce the formation of secondary radiation. PE is a viable option for shielding because of its high H content and low weight. PE loaded with another element (like boron or lithium) would enhance performances because of improved structural integrity and shielding against other radiation types (neutrons for example).

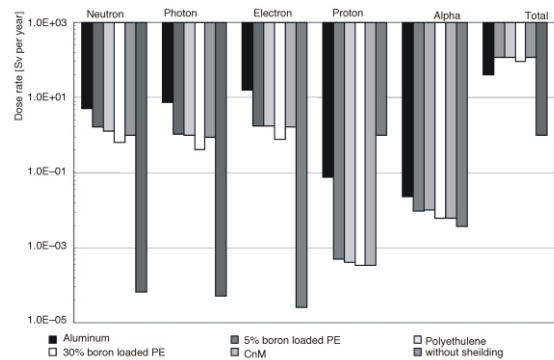


Figure 8. MCNPX dose rates from 100 MeV proton source without shielding, 3.7 cm of Al, 10.55 cm 5% boron loaded PE, 8.33 cm 30% boron PE, and 10.55 cm CnM

Table 4. With-to-without shielding dose ratio: 100 MeV proton energy; intensity .4 protons/s-cm²-sr-MeV per nucleon; dose without shielding 0.0932 Sv per year¹

Material	Thickness [cm]	Neutron	Photon	Electron	Proton	Alpha	Total
Aluminum	3.7	5.06E+00	7.55E+00	1.58E+01	7.71E-02	2.34E-02	4.02E+01
Polyethylene	10.55	1.31E+00	1.02E+00	1.74E+00	4.16E-04	9.78E-03	1.14E+02
5% boron loaded PE	10.55	1.67E+00	1.04E+00	1.73E+00	4.82E-04	9.64E-03	1.14E+02
30% boron loaded PE	8.33	6.37E-01	4.00E-01	7.74E-01	3.45E-04	6.08E-03	9.03E+01
CnM	10.55	9.79E-01	8.74E-01	1.68E+00	3.32E-04	6.01E-03	1.14E+02
Without any shielding	–	6.77E-05	5.22E-05	2.53E-05	9.96E-01	3.67E-03	1.00E+00

Table 5. Volume and mass density of hydrogen in various shielding materials [19]

Material	H (liquid)	LiH	PE	Water	PAH	CnM
Density [gcm ⁻³]	0.07	0.78	0.92	1.0	10	*
wt.% H	100	12.7	14.3	11.2	1-4	>20
Atom % H	100	50	67	67	>30	<30
H density [10 ²² cm ⁻³]	5.3	5.9	7.9	6.7	20	*

* No available data

The total dose rate from 100 MeV protons without shielding is obtained to be 0.0932 Sv per year. The dose rate from protons is 0.996 of the overall dose without shielding; the aluminum gives a 0.07 reduction from the proton dose without shielding. Table 4 shows the dose rate ratios for the analyzed materials indicating that the best shielding materials are: 30% boron loaded polyethylene, followed by the nano-carbon fibers, 5% boron loaded polyethylene, and aluminum.

High energy alpha particles

Theoretical consideration. Alpha particles from the cosmic radiation are in the energy range from 5 MeV per nucleon to over GeV per nucleon. However, the expected flux of high energy alphas from space is much smaller than that of high energy protons. In survey studies, therefore, the effect from alphas as primary sources may be neglected and the protons from cosmic radiation could be considered as the only source. In addition, greater thicknesses are necessary to shield high energy protons (because they are lighter than alphas); the expected density thickness is around 20 g/cm². However, alphas are considered in this analysis in order to verify that they can also be shielded by the same shielding materials used for protons.

The PE is considered to be the best “standard” shielding material not only because of its efficiency

to stop various types of radiation but also from the point of manufacturing and durability. Further studies on spacecraft shielding also demonstrate that higher *Z* materials are worse not only because they have a lower shielding efficiency but also because they increase the dose rates due to the production of secondary radiation. On the other hand, Adams *et al.*, from NASA, propose some “novel” materials. These materials are: carbon nano-materials (CnM), lithium hydride (LiH), hydrogen-charged palladium/silver alloys (Pd/Ag/H or PAH), and borated polyethylene (BPE) [2]. The carbon nano-materials contain H up to 20 wt%. LiH is competitive with PE in shielding against the cosmic rays due to similar H content. The PAH materials have higher volumetric H density; they may have dual-use applications. The BPE material adds to PE properties a larger neutron capture capability. The properties of these materials related to hydrogen content are listed in tab. 5. H and water are also included for comparison.

Figures 9 and 10 show the linear and density CSDA ranges for different materials as a function of alpha particle energies. In addition, pure H and C are considered as well, since they are main constituent elements of the analyzed shielding materials. From fig. 9 it can be seen that thicknesses for stopping alphas of more than 1 GeV must be larger than 10 cm. However, in the energy range of interest, the shielding thickness is in the range of just a few centimeters. The density range shown in fig. 10 for various shielding candidate materials is compared with the thickness of 20 g/cm² that corresponds to the thickness used at the International Space Station. It is accepted that this thickness will produce no sig-

¹ The thickness of the material analyzed corresponds to the density range at 100 MeV that would stop all incoming protons

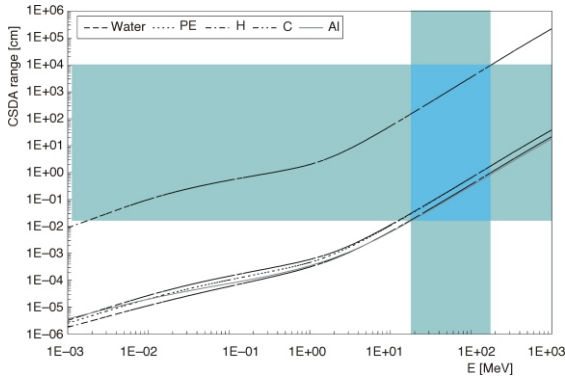


Figure 9. Linear CSDA range of α -particles vs. energy for H, water, C, PE, and Al

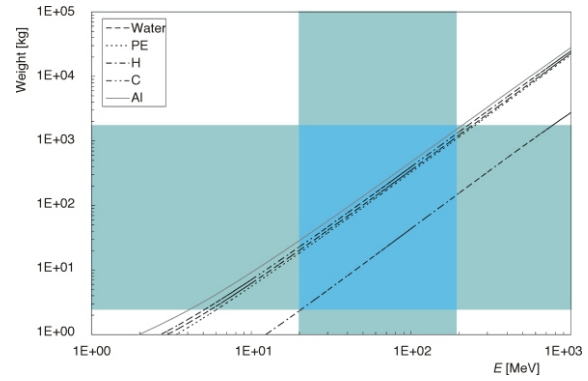


Figure 11. Weight of shielding materials for a room of 5 5 3 m and a thickness of CSDA range as a function of alpha particle energy

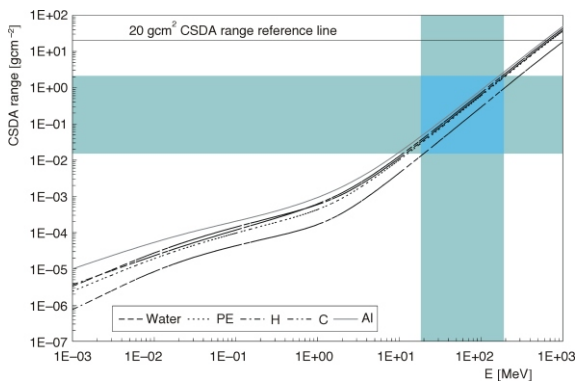


Figure 10. Density range of α -particles vs. energy for H, water, C, PE, and Al

nificant secondary radiation for protons, the highest contributor to cosmic rays. Because of the production of secondary radiation, thicknesses greater than this are not suggested (shielding efficiency is maintained almost constant while weight is increased). Among the analyzed shielding materials, aluminum gives the highest shielding weight for the same shielding efficiency. For alphas of 200 MeV the CSDA range in Al material is 3 g/cm². This range is

expected to be greater than for other materials. Therefore, the thickness with the value of this range is selected to compare other materials.

Figure 11 shows that shielding weights for a spacecraft room of 5 5 3 m and energies of the alpha particles above GeV are around dozens of tons which is not acceptable (since the whole spacecraft weight would be expected to be around that value). On the other hand, for energies in the range of interest (up to 200 MeV), the weights are below the tons, giving more promising selections.

Numerical analysis. For the energies of alpha particles in the order of 200 MeV, the shielding thickness must not be smaller than 3 g/cm². The materials considered in numerical study are PE, BPE, CnM, LiH, and Pd/Ag/H. The numerical model is shown in fig. 4. The case without the shielding assumes only detector. The resulting total dose in that case is 9 mSv per year, representing 4.5% of the 200 mSv per year limit. Table 6 shows the with-to-without shielding dose ratios for various shielding materials. It can be seen that all shielding materials but PAH give a significant reduction in dose rate. However, none of the novel materials improved the efficiency of PE. CnM shows a slight

Table 6. With-to-without shielding dose ratio: 200 MeV alpha energy; intensity 4 10⁻⁵ alphas/s-cm²-sr-MeV per nucleon; 9 mSv per year dose without shielding

Material	Neutron	Photon	Electron	Proton	Alpha	Total
LiH	2.E+00	8.E-02	1.E-01	4.E-01	2.93.E-05	1.48.E-03
BPE	1.E+00	4.E-01	8.E-01	3.E-01	2.40.E-05	1.22.E-03
CnM	1.E+00	4.E-01	7.E-01	3.E-01	1.60.E-05	1.02.E-03
PAH	3.E+00	3.E+00	5.E+00	9.E-01	1.26.E+00	1.26.E+00
PE	1.E+00	4.E-01	8.E-01	3.E-01	1.87.E-05	1.14.E-03
Al	2E+00	2E+00	4E+00	4E-01	7.52.E-03	8.94.E-03
Without any shielding	1.E-05	8.E-07	4.E-07	3.E-03	9.96.E-01	1.00.E+00

and non significant improvement and only under the assumptions that it contains 20 wt.% H with the density similar to PE.

In order to verify the shielding performances of the above materials for different energies of alpha particles, 20 MeV and 2 GeV are selected. For 2 GeV alphas, intensity is that of GCR maximum (conservative approach: $4 \cdot 10^{-5}$ alphas/s-cm²-sr-MeV per nucleon). In these cases the total dose without shielding reaches 0.3 mSv per year and 650 mSv per year, respectively. Therefore, a reduction to less than a 30% is required to stay under 200 mSv per year limit for higher alpha energies. For 20 MeV no change is required. Tables 7 and 8 show the comparison of efficiency of different materials for 20 MeV and 2 GeV alpha particles. For 2 GeV alpha particles, the minimum required reduction is not achieved. Since the used intensity for this energy is equal to that of the whole GCR flux, it is expected to have much smaller dose than obtained. For alphas of 20 MeV, it can be observed that the BPE presents some improvement in respect to PE. In all cases, it can be understood that Al is fairly the least efficient. Thus the thickness of 3 g/cm² seems acceptable for materials such as PE, CnM, BPE (3 cm) and LiH (4 cm). With this value, the weight of a room with the dimensions abovementioned would reach nearly 2 tons. However, a 20 g/cm² thick shielding is analyzed to take

into account shielding against protons which penetrate longer distances than alphas of same energies. The following multi-slab geometry was tested: facing the source, a layer of 5 cm Al (simulating the spacecraft wall) corresponding to 13.5 g/cm² followed by 6.85 cm PE that corresponds to 6.5 g/cm²

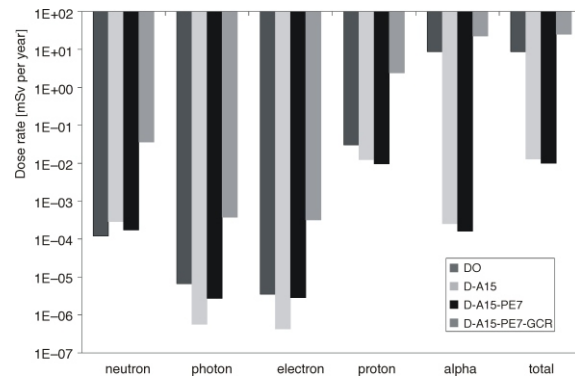


Figure 12. MCNPX dose rate from alpha (intensity 50 MeV per nucleon – $4 \cdot 10^{-5}$ alphas/s-cm²-sr-MeV per nucleon without shielding (D0), with 5 cm of Al plus 6.85 cm PE (D-A15-PE7), and a GCR-like alpha source (intensity 500 MeV per nucleon – $4 \cdot 10^{-5}$ alphas/s-cm²-sr-MeV per nucleon) with 5 cm Al and 6.85 cm PE shielding (D A15-PE7-GCR)

Table 7. With-to-without shielding dose ratio; 20 MeV alpha energy; intensity $4 \cdot 10^{-5}$ alphas/s-cm²-sr-MeV per nucleon; 0.3 mSv per year dose without shielding

Material	Neutron	Photon	Electron	Proton	Alpha	Total
LiH	5.E-01	2.E-02	0.E+00	2.E-03	0.00.E+00	1.70.E-07
BPE	2.E-01	2.E-01	0.E+00	0.E+00	0.00.E+00	8.45.E-09
CnM	5.E-02	1.E-01	1.E-01	0.E+00	0.00.E+00	3.70.E-09
PAH	4.E-01	2.E-01	2.E-01	4.E-04	0.00.E+00	4.09.E-08
PE	2.E-01	2.E-01	3.E-02	0.E+00	0.00.E+00	8.89.E-09
Al	9.E-01	8.E-01	6.E+01	2.E-03	0.00.E+00	1.50.E-07
Without any shielding	3.E-08	6.E-09	1.E-08	6.E-05	1.00.E+00	1.00.E+00

Table 8. With-to-without shielding dose ratio; 2 GeV alpha energy; intensity $4 \cdot 10^{-5}$ alphas/s-cm²-sr-MeV per nucleon; 650 mSv per year dose without shielding

Material	Neutron	Photon	Electron	Proton	Alpha	Total
LiH	4.E+00	2.E+00	2.E+00	3.E+00	9.08.E-01	9.29.E-07
BPE	4.E+00	2.E+00	2.E+00	3.E+00	9.11.E-01	9.32.E-01
CnM	4.E+00	2.E+00	2.E-00	3.E+00	9.04.E-01	9.25.E-01
PAH	6.E+00	8.E+00	2.E-01	3.E+00	9.61.E-01	9.80.E-01
PE	4.E+00	2.E+00	2.E-00	3.E+00	9.08.E-01	9.29.E-01
Al	5.E+00	6.E+00	1.E+01	3.E+00	9.42.E-01	9.64.E-01
Without any shielding	8.E-05	9.E-07	5.E-08	1.E-02	9.89.E-01	1.00.E+00

is added. Figure 12 shows the dose rate distribution in the shield. It can be seen that without the shielding the total dose is mainly due to alphas and it is not larger than the limit. The Al layer drastically reduces alpha dose but makes secondary radiation. The addition of PE layer reduces secondary radiation. Therefore, the total dose at the inner side of PE layer is below the 200 mS per year limit.

High and low energy photons

Theoretical consideration. Although high energy photons present energetic and penetrating source of radiation, their abundances in space radiation field are low and therefore they are not considered as primary radiation. However, photons are produced as secondary radiation and this section therefore reviews the best selection of light materials for shielding against high and low energy photons. Photon interactions with materials take place through the photoelectric effect, Compton scattering, and pair production. The photoelectric effect is the dominant form of energy transfer at low photon energies and low Z materials. Pair production is considered to be a main form of energy deposition at assumed average energy of 1 GeV important for space shielding design. High energy photons (gamma rays) are best shielded by higher Z materials such as lead; however, due to their high density, high Z materials such as lead remain an unacceptable choice for shielding of the space craft.

As an illustration we present the analysis of the 1 MeV photon interactions with various materials. The mass attenuation coefficients μ_m , for 1 MeV gamma rays are very similar for water, PE, Pb, Al, B, and Li and are higher for H (tab. 9). Mass attenuation coefficients allow analyzing the impact of material density, ρ , in regards to the gamma ray attenuation. This is shown by the intensity relationship:

$$\frac{I}{I_0} = e^{-\mu_l x_l}$$

or

$$\frac{I}{I_0} = e^{-\mu_m \rho x_l}$$

where I/I_0 represents the ratio of intensity with and without the shielding (penetration coefficient), μ_l is the (linear) thickness of the shielding material, and x_l is the linear attenuation coefficient. Another interesting expression to consider is:

$$\frac{I}{I_0} = (e^{-\mu_m x_l})^\rho$$

which implies that for equal $\mu_m x_l$, penetration is a negative exponential function of material density. Figure 13 shows an I/I_0 trend against x_l and it can be seen that differences in penetration for the same thicknesses are very significant for different density materials. This effect can also be observed in linear attenuation coefficients, shown in tab. 9. The impact can be followed by comparing the coefficients normalized to lead. While the ratios for μ_m are near 100%, except for the hydrogen with a greater ratio, the ratios for μ_l are all under 24%, with the exception for the Pb.

Finally, it can be concluded that the penetration decreases exponentially as material density increases. This means that the higher density materials are better for shielding (by comparison of similar μ_m). This behavior also implies that when $\mu_m x_l < 1$ differences in ρ have a greater impact on I/I_0 ; inversely, when $\mu_m x_l \gg 1$, changes in density do not have so much influence in penetration or attenuation, $1 - I/I_0$. Although “the thicker shielding, the better” is a true statement, its validity depends on other conditions and criteria. In designing the space shuttle shielding, for instance, there are two problems arising with the increasing thickness of the shielding: size and weight. These two factors are important for determining the material as well as its shielding capability. By optimizing the size and weight and the material efficiency, an effective shield can be found. In respect to size, it is necessary to select the desired penetration ratio while maintaining a reasonable thickness of a shield, *i. e.* selecting the material with the smallest linear mean free path: $\mu_l = 1/\mu_l$. The same principle applies for the

Table 9. Attenuation coefficients and densities for H, water, PE, Pb, Al, B, and Li, and their ratios to Pb

	H	Water	PE	Pb	Al	B	Li
μ_m [cm ² g ⁻¹]	0.13	0.07	0.07	0.07	0.06	0.06	0.06
μ_m/μ_{mPb}	178%	100%	102%	100%	87	83%	77%
μ_l [cm ⁻¹]	1.06E-05	7.07E-2	6.82E-2	8.05E-01	1.66E-01	1.40E-01	2.94E-02
μ_l/μ_{lPb}	0%	9%	8%	100%	21%	17%	4%
ρ [gcm ⁻³]	0.0000837	1	0.94	11.34	2.7	2.37	0.534
ρ/ρ_{Pb}	0%	9%	8%	100%	24%	21%	5%

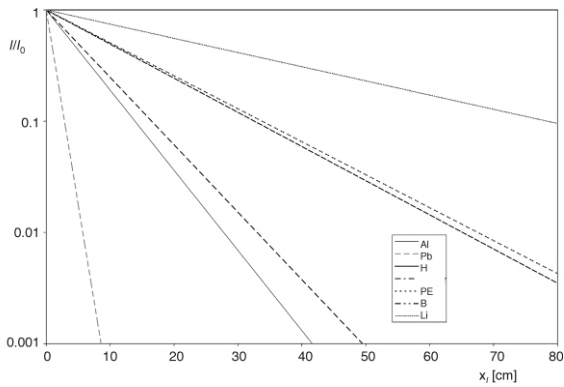


Figure 13. Penetration of 1 MeV photons vs. linear thickness for Al, Pb, H, water, PE, B, and Li

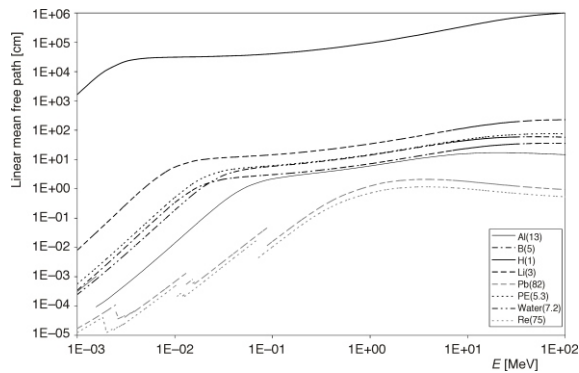


Figure 14. Linear mean free path of photons vs. energy for Al, B, H, Li, Pb, PE, water, and Re

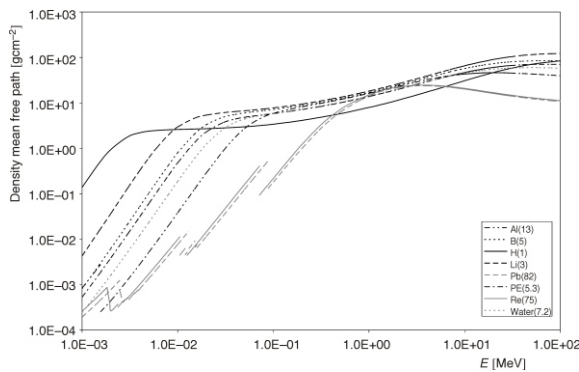


Figure 15. Density mean free path of photons vs. energy for Al, B, H, Li, Pb, PE, water, and Re

weight criterion; however, the variable is now the unit mass, not shielding thickness; the material with the smallest density mean free path, $\mu_m = 1/\mu_m$ will prove to be the most efficient one.

Figures 14 and 15 show respectively the trends of the linear and density mean free paths as a function

of photon energy for H, water, PE, Al, B, Li, Pb, and Re. The Pb and Re are both included as control materials considering their high capabilities to stop neutrons and gamma rays. The linear mean free paths for these materials show a general behavior: they are higher for lower Z materials. Re is the exception and its high density, 21 g/cm^3 , is one of the main reasons. All μ_1 increases with energy in the range analyzed; those of Pb, and Re reach a maximum at 3 MeV. Clearly, this trends show that the material which requires a smallest thickness is Re while H is the one that requires the thickest shielding. The maximum ratio between μ_1 of different materials is around 10^9 . The density mean free path curves show that Pb is the material that requires less mass for the same shielding efficiency in the gamma ray energy range of interest. However, around 1 MeV, the most mass-effective material is H, while it is the least effective under 0.01 MeV. At this energy all density mean free paths are in the order of a semi-order of magnitude of difference. The maximum ratio between μ_m of different materials is around 10^4 . Re and Pb behave very similarly. In conclusion, the materials selected for making the smallest and lightest shielding are Re or Pb. For energies around 1 MeV, H is selected under the weight criterion.

Numerical analysis. The desired shield thickness is estimated using the model shown in fig. 4 and adopting the design criteria for shielding against gamma of the incoming gamma ray intensity reduction to 10%. The results are shown in tab. 10 and can be compared visually in fig. 16¹. It can be easily observed that several materials are good gamma absorbers requiring small thickness and therefore small weight. These materials are aluminum, silicon, copper, silver, cesium, gadolinium, hafnium, rhenium, osmium, lead, and hydrogen.

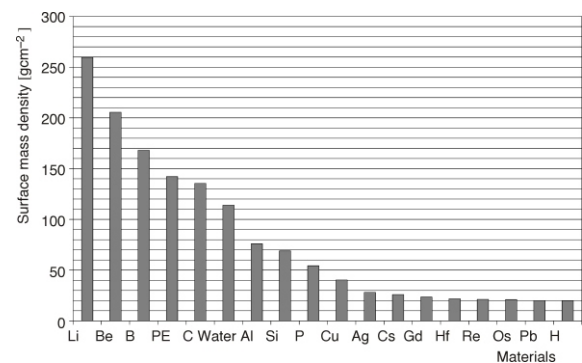


Figure 16. Comparison of how much surface mass is needed to decrease the initial intensity of 1 GeV gamma rays to 10%

¹ Surface mass density is defined as the thickness of the material multiplied by its density

Table 10. Materials analyzed for shielding against gamma rays

Material	Density [gcm ⁻³]	Mass attenuation coefficient [cm ² g ⁻¹]	Linear attenuation coefficient [cm ⁻¹]	Thickness [cm]	Surface mass density [gcm ⁻²]
Li	0.530	0.009	0.005	489.797	259.592
Be	1.850	0.011	0.021	111.129	205.588
B	2.370	0.014	0.032	70.916	168.072
PE	0.940	0.016	0.015	151.207	142.135
C	2.260	0.017	0.038	59.932	135.446
Water	1.000	0.020	0.020	113.989	113.989
Al	2.700	0.030	0.082	28.146	75.993
Si	2.330	0.033	0.078	29.588	68.940
P	1.820	0.042	0.077	29.839	54.306
Cu	8.960	0.057	0.513	4.493	40.255
Ag	10.500	0.082	0.861	2.674	28.080
Cs	1.870	0.089	0.166	13.866	25.930
Gd	7.900	0.098	0.777	2.965	23.424
Hf	13.310	0.106	1.411	1.632	21.723
Re	21.040	0.109	2.293	1.004	21.125
Os	22.600	0.110	2.486	0.926	20.933
Pb	11.350	0.115	1.305	1.764	20.022
H	8.37E-05	0.116	0.000	237154.976	19.850

However, several of these materials cannot be considered for missions to deep space due to availability, cost, and the thickness they require, and those are Os, Re, Ag, Hf, and H. For example, an H shield thickness of approximately 237 meters is needed, which indeed is not feasible for a space craft. The linear thickness of the selected materials for shielding gamma rays needed to reduce the incoming gamma rays of 1 GeV is compared in fig. 17. As it can be seen, a very small amount of Pb, Gd, and even Cu can be used against gamma rays. However, the most important aspects to analyze are the physical and chemical properties of the materials as well

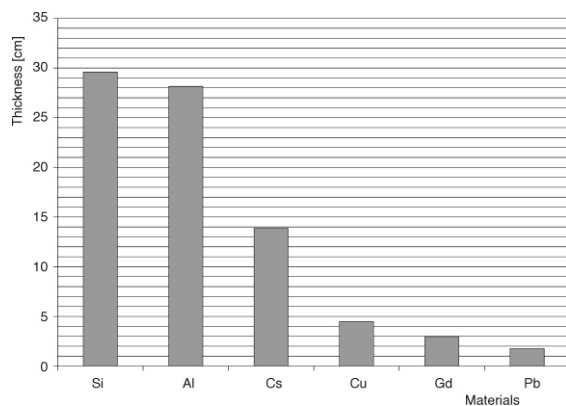


Figure 17. Comparison of linear thickness required to decrease the initial intensity of a 1 GeV gamma ray to 10% for selected materials

as the secondary radiation these materials will produce after primary gamma rays of 1 GeV pass through. Silicon is a very brittle material and as such it might not be a good shielding material. Although chemically active, cesium can be used by introducing rigorous safety criteria of isolating the cesium layer from the crew. Figure 18 shows the number of events and potential secondary radiation from the selected materials after the primary gamma rays pass through. Most of the interactions are photoelectric absorptions and Compton effects which leads to a stream of electrons and secondary gamma radiation. The comparison of energy depositions due to all interactions in selected materials is depicted in fig. 19.

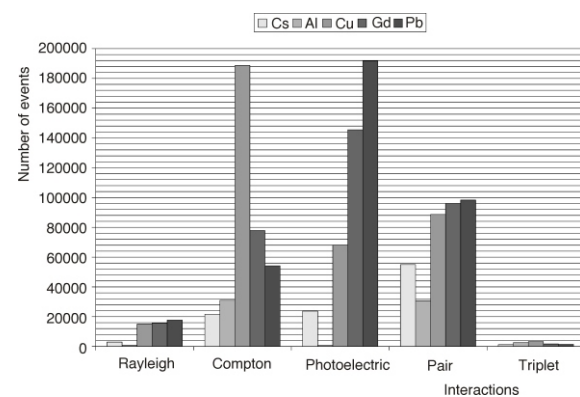


Figure 18. Comparison of number of events (density) for selected materials

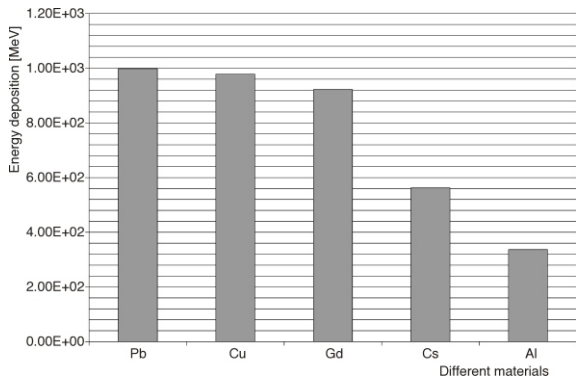


Figure 19. Comparison of energy deposited in selected materials after interaction with 1 GeV gamma rays

The high Z materials are the best in shielding against gammas. However, these materials are not favorable due to enormous amount of secondary radiation produced and the corresponding weight. The materials such as aluminum, copper, silicon, and cesium can be used. The design area (thickness vs. attenuation) is shown in fig. 20. As it can be observed, the required thickness to attenuate 90% of the 1 GeV gammas for Al, Cs, Cu, and Si are 47.4, 19.3, 7, and 49.2 cm, respectively.

High and low energy electrons

Electrons are not found to be primary source of radiation in space. Their importance comes from their appearance as trapped electrons in planet magnetic fields, with energies of 4 up to 7 MeV. They also appear as secondary radiation. It implies that their highest energy will be up to the maximum energy of the space radiation, *i. e.* the energies above GeV.

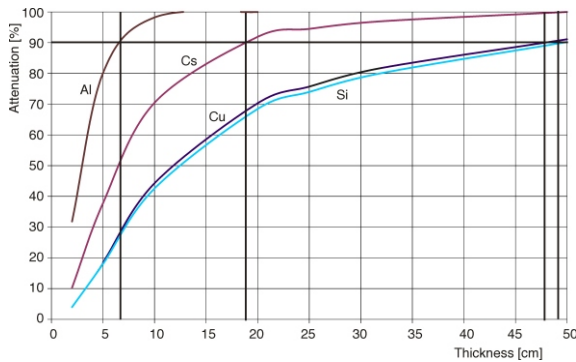


Figure 20. Design area for primary high energy gamma rays: the thickness cut-off for 90% attenuation of the 1 GeV gamma rays

Same materials as analyzed in previous sections are therefore considered to estimate the efficiency against high energy electrons: polyethylene (PE), boron-loaded polyethylene (BPE), carbon nano-materials (CnM), lithium hydride (LiH), and hydrogen-charged palladium/silver alloys (Pd/Ag/H or PAH). In order to analyze shielding for such particles, linear and density ranges for a wide range of energies and for various materials are assessed. Figures 21 and 22 show a plot of linear and density ranges for the electrons of various energies and for various materials.

From these two figures it can be seen that the lighter shielding would be made of H and Ag, for electron energies below and above 100 MeV respectively, while the smallest thickness is obtained for Pd. In order to avoid secondary radiation, it is desired to have the material with the lowest Z, in this case it is H. PE is a very good alternative under criteria of weight, size and secondary produced radiation. Below 10 MeV, more probable energy than 1 GeV, the PE shielding becomes the lightest in addition to H. For 7 MeV electrons, the maxi-

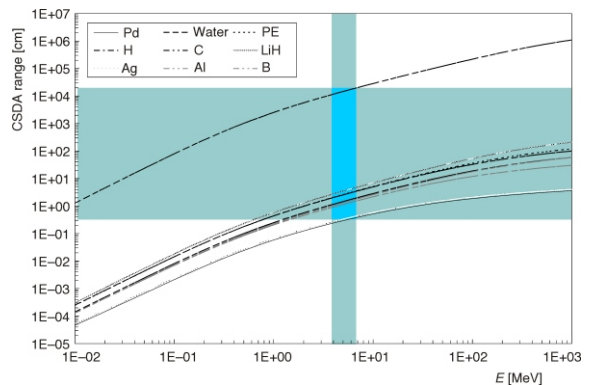


Figure 21. CSDA linear range of electrons vs. energy for H, water, C, PE, Al, LiH, Pd, Ag, and B

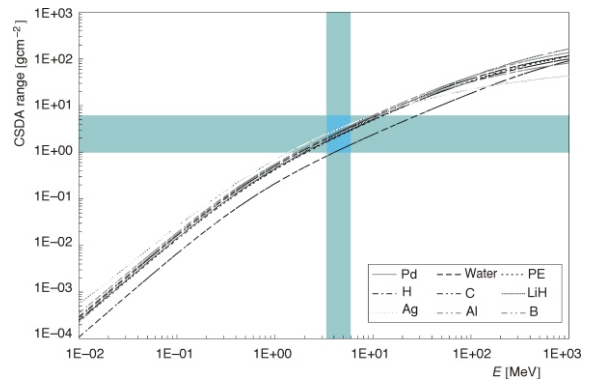


Figure 22. Density range of electrons vs. energy for H, water, C, PE, Al, LiH, Pd, Ag, and B

mum range would be 5 g/cm² for Ag. Therefore, if a thickness with this value is considered, the other materials would have the overrange thickness. The weight of a room of 5 × 5 × 3 m would be a few tons. Thus PE is selected as one of the best electron-shielding materials for spacecrafts.

High and low energy neutrons

Theoretical consideration. High energy neutrons must be slowed before they can be captured through inelastic scattering with high Z materials or elastic scattering with low Z materials. Neutrons are most effectively shielded at all energies by a material that is close to their mass, namely the hydrogen nucleus. Therefore, dense compounds of low Z atoms are preferred. Neutrons are not main constituents of primary space radiation but they will be created through spallation. This event occurs when highly energetic protons collide with the atoms of various materials ejecting many neutrons of high energy. This secondary radiation source of neutrons must be attenuated with an additional neutron-shielding material. The most common polymer that shows great potential in shielding against neutrons is PE. A number of different PEs is available: pure PE, 7.5% lithium loaded PE, 5% boron loaded PE, and 30% boron loaded PE. Boron and lithium loaded PE have very high neutron cross sections at low and high energies. The density of the selected PE materials in comparison with aluminum are show in tab. 11.

Table 11. Polyethylene and aluminum densities

Material	[gcm ⁻³]
5% boron loaded PE	0.9
30% boron loaded PE	2.52
7.5% lithium loaded PE	1.03
Pure PE	0.94
Aluminum	2.7

Numerical analysis. Neutron transport analysis was performed using the same geometry as shown in fig. 4. Modeling was performed using the COG Monte Carlo code. The maximum neutron energy is restricted by the data available in the cross-section libraries used by the COG. Selected neutron energies ranged from 5 to 30 MeV. Figures 23 to 28 show the neutron attenuation through selected materials for different neutron energies and material thicknesses. It can be seen that the 30% boron loaded PE has good shielding response to highly energetic neutrons. Moreover, to slow the neutrons to thermal energies it would take far less thickness than using any

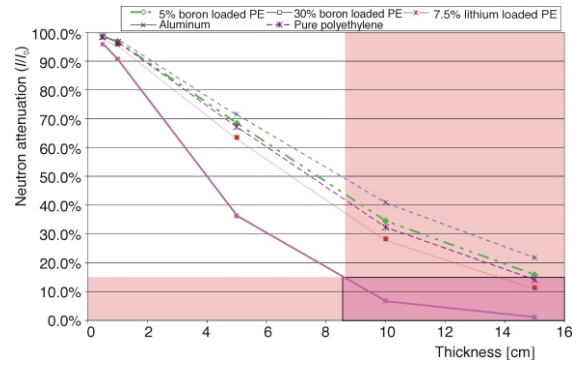


Figure 23. Neutron attenuation vs. thickness for different materials at 5 MeV

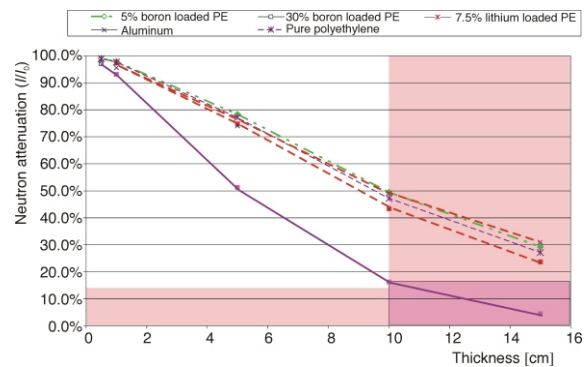


Figure 24. Neutron attenuation vs. thickness for different materials at 10 MeV

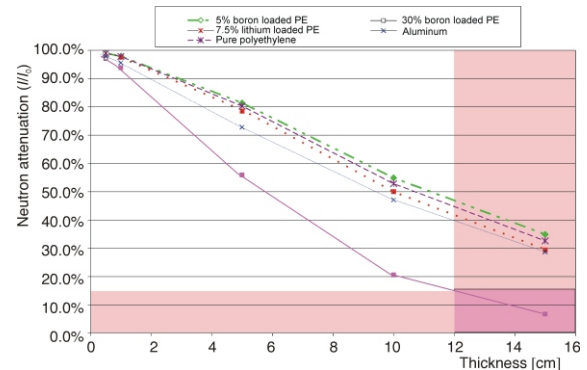


Figure 25. Neutron attenuation vs. thickness for different materials at 15 MeV

other of the selected materials. A satisfactory attenuation value of 15% of the initial energy was tentatively adopted as a criterion to compare the efficiency of selected materials. The highlighted area indicates the thickness required to achieve this neutron attenuation. Numerical values of the attenuation decrements and neutron energy reduction after shielding materials are summarized in tabs. 12 and 13, respectively. The results point at 30% boron loaded PE as the best candidate material.

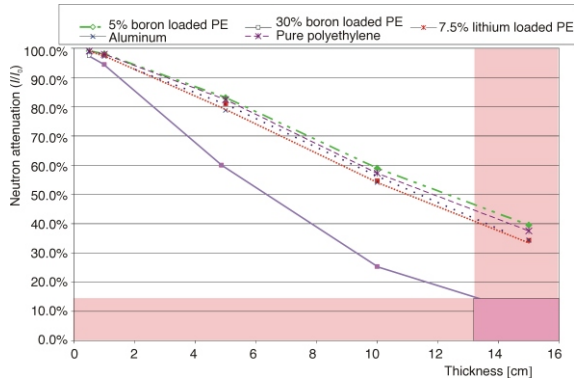


Figure 26. Neutron attenuation vs. thickness for different materials at 20 MeV

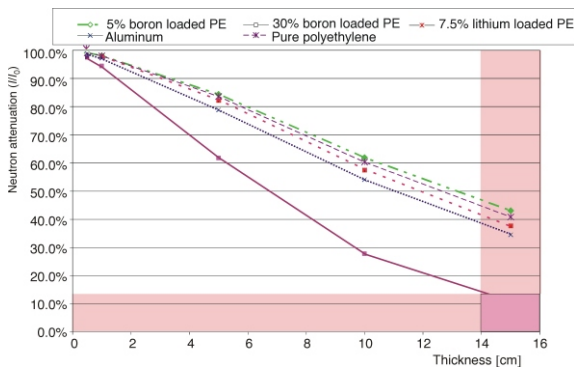


Figure 27. Neutron attenuation vs. thickness for different materials at 25 MeV

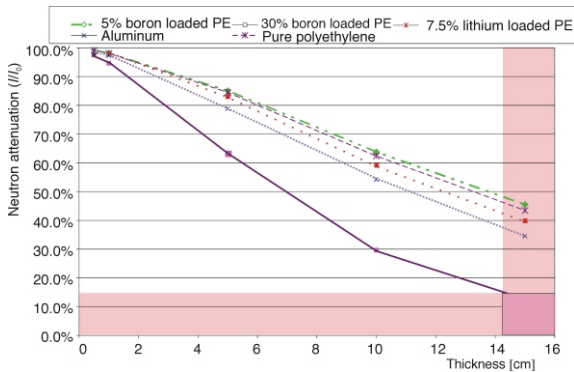


Figure 28. Neutron attenuation vs. thickness for different materials at 30 MeV

Preliminary model: spacecraft room and shielding design

According to the discussion with NASA experts, the living area of astronauts is modeled as a room shown in fig. 29. The size of the room is set to 5 5 3 m. The interior of the room is filled with air. A numerical simulation model includes the distribu-

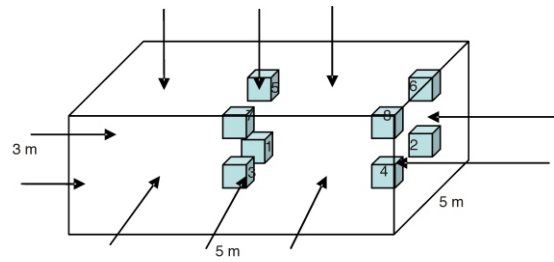


Figure 29. MCNPX spacecraft room model with eight detector positions

tion of detectors (selected dimension is 1/10 of the room size, *i. e.* 0.5 0.5 0.3 m) that are used to analyze the flux distribution in the room.

The detector is assumed to be made of pure water. Due to the symmetry of the room, the detectors are placed at eight different positions as shown in fig. 29. As already described protons and alphas are the two main constituents of primary space radiation field. This space radiation field was assumed to be isotropic around the spacecraft room. Since the nature of SPEs is still unpredictable, only GCR was included in this stage of modeling. The intensity and energy spectrum of radiation particles, protons and alphas, were based on the data shown in fig. 1. The criterion for the ISS of 20 g/cm² was adopted as density thickness of the composite spacecraft room shielding. Aluminum has always been used to manufacture spacecrafts and therefore it is assumed also in this analysis as a material that will be used to manufacture the spacecraft room. Aluminum is also a good material to shield against photons according to the previous analysis. The numerical analyses on shielding against high energy proton and alpha particles showed that PE is a good material. Therefore, the combination of 0.5 cm Al and 20 cm PE was selected to calculate the annual dose distribution in the spacecraft room (see fig. 30). The total linear density of this combination of materials is 20.3 g/cm².

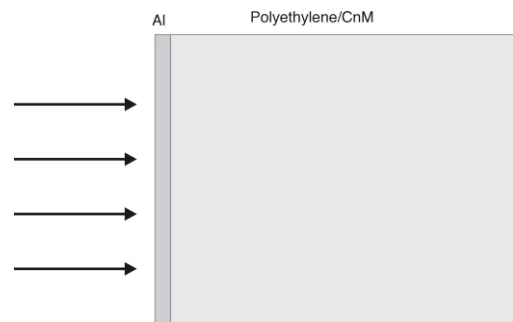


Figure 30. Shielding combination

Table 12. Neutron attenuation for a variety of materials, energies, and thicknesses

Neutron response					
5 MeV					
Shield thickness [cm]	5% boron loaded polyethylene	30% boron loaded polyethylene	7.5% lithium loaded polyethylene	Aluminum	Pure polyethylene
0.5	98.6%	95.8%	98.2%	98.1%	98.5%
1	96.8%	90.6%	95.9%	95.9%	96.5%
5	68.5%	36.3%	63.6%	71.6%	67.2%
10	34.5%	6.8%	28.4%	41.0%	32.3%
15	15.9%	1.1%	11.4%	21.8%	14.2%
10 MeV					
0.5	99.0%	97.0%	98.7%	97.9%	99.0%
1	97.8%	93.2%	97.4%	95.6%	97.7%
5	78.3%	51.2%	74.8%	74.1%	77.1%
10	49.4%	16.2%	43.4%	49.1%	47.2%
15	29.2%	4.4%	23.7%	30.9%	27.1%
15 MeV					
0.5	99.0%	97.1%	98.9%	97.8%	99.0%
1	97.9%	93.8%	97.6%	95.6%	97.8%
5	81.4%	55.9%	78.5%	72.9%	80.3%
10	54.9%	20.6%	50.0%	47.2%	52.8%
15	34.9%	6.7%	29.4%	28.7%	32.6%
20 MeV					
0.5	99.1%	97.5%	99.0%	98.8%	99.1%
1	98.1%	94.5%	97.8%	97.2%	98.0%
5	83.1%	60.0%	81.1%	78.8%	82.4%
10	59.0%	25.3%	54.7%	54.2%	57.2%
15	39.5%	9.4%	34.3%	34.5%	37.5%
25 MeV					
0.5	99.1%	97.5%	99.0%	98.8%	99.1%
1	98.1%	94.4%	97.8%	97.3%	98.0%
5	84.4%	61.7%	82.2%	78.9%	83.6%
10	61.9%	27.7%	57.5%	54.1%	60.3%
15	43.1%	11.0%	37.7%	34.6%	40.8%
30 MeV					
0.5	99.2%	97.5%	99.0%	98.8%	99.1%
1	98.1%	94.6%	97.9%	97.3%	98.0%
5	85.1%	62.8%	83.1%	78.9%	84.5%
10	63.8%	29.7%	59.2%	54.2%	62.3%
15	45.5%	12.6%	39.8%	34.6%	43.4%

The equivalent annual dose distribution in the spacecraft room is shown in tab. 14. The dose is highest at the corner of the room (position 8, fig. 29). This value is much higher than the allowed dose level; other locations show much lower dose rates. For example, the equivalent dose rates at position 6 and 7 (fig. 29) were the lowest, and the closest to the safe level of the International Space

Station, 200 mSv per year. Table 14 also shows the contribution of different kinds of radiation (including the secondary radiation) to the total dose level. Protons contribute 81~87% to the total dose, alphas contribute around 10%, and the secondary neutrons give additional 5%. The dose rates due to the secondary photons and electrons are relatively low (on average below 1%).

Table 13. Neutron energy after shielding for a variety of materials, energies, and thicknesses

Energy transmittion					
5 MeV					
Shield thickness [cm]	5% boron loaded polyethylene	30% boron loaded polyethylene	7.5% lithium loaded polyethylene	Aluminum	Pure polyethylene
0.5	4.93E+00	4.79E+00	4.91E+00	4.90E+00	4.93E+00
1	4.84E+00	4.53E+00	4.80E+00	4.79E+00	4.83E+00
5	3.42E+00	1.81E+00	3.18E+00	3.58E+00	3.36E+00
10	1.73E+00	3.38E-01	1.42E+00	2.05E+00	1.61E+00
15	7.93E-01	5.28E-02	5.70E-01	1.09E+00	7.09E-01
10 MeV					
0.5	9.90E+00	9.70E+00	9.87E+00	9.79E+00	9.90E+00
1	9.78E+00	9.32E+00	9.74E+00	9.56E+00	9.77E+00
5	7.83E+00	5.12E+00	7.48E+00	7.41E+00	7.71E+00
10	4.94E+00	1.62E+00	4.34E+00	4.91E+00	4.72E+00
15	2.92E+00	4.41E-01	2.37E+00	3.09E+00	2.71E+00
15 MeV					
0.5	1.49E+01	1.46E+01	1.48E+01	1.47E+01	1.48E+01
1	1.47E+01	1.41E+01	1.48E+01	1.43E+01	1.47E+01
5	1.22E+01	8.39E+00	1.18E+01	1.09E+01	1.20E+01
10	8.24E+00	3.09E+00	7.51E+00	7.07E+00	7.92E+00
15	5.23E+00	1.01E+00	4.42E+00	4.31E+00	4.89E+00
20 MeV					
0.5	1.98E+01	1.95E+01	1.98E+01	1.98E+01	1.98E+01
1	1.96E+01	1.89E+01	1.96E+01	1.94E+01	1.96E+01
5	1.66E+01	1.20E+01	1.62E+01	1.58E+01	1.65E+01
10	1.18E+01	5.06E+00	1.09E+01	1.08E+01	1.14E+01
15	7.90E+00	1.88E+00	6.86E+00	6.90E+01	7.51E+00
25 MeV					
0.5	2.48E+01	2.44E+01	2.47E+01	2.47E+01	2.48E+01
1	2.45E+01	2.36E+01	2.45E+01	2.43E+01	2.45E+01
5	2.11E+01	1.54E+01	2.06E+01	1.97E+01	2.09E+01
10	1.55E+01	6.94E+00	1.44E+01	1.35E+01	1.51E+01
15	1.08E+01	2.74E+00	9.42E+00	8.64E+00	1.02E+01
30 MeV					
0.5	2.97E+01	2.92E+01	2.97E+01	2.96E+01	2.97E+01
1	2.94E+01	2.84E+01	2.94E+01	2.92E+01	2.94E+01
5	2.55E+01	1.88E+01	2.49E+01	2.37E+01	2.53E+01
10	1.91E+01	8.90E+00	1.78E+01	1.62E+01	1.87E+01
15	1.36E+01	3.79E+00	1.20E+01	1.04E+01	1.30E+01

In addition, a carbon nano-material (CnM) is analyzed. As already introduced, the density of CnM can be adjusted, thus storing a large amount of hydrogen within the nano-structure, which makes it effective in shielding against the protons and neutrons. The previous survey study was based on CnM with only 20% weight of hydrogen. A newly developed CnM which can store

67% weight of hydrogen [20] was used in this simulation to compare the efficiency of the shielding against the space radiation field. The equivalent annual dose rates with the shielding of 0.5 cm Al and 20 cm CnM were shown in tab. 15. The density of the CnM is the same as that of PE, so the total density of the shielding is kept the same, 20.3 g/cm². In this case, the protons contribute

Table 14. Equivalent annual dose rates [mSv per year] in the spacecraft model room with the wall made of 0.5 cm Al and 20 cm PE

Position (fig. 29)	Proton	Alpha	Photon	Electron	Neutron	Total
1	470.44	78.47	0.58	0.44	27.86	578
	81.4%	13.6%	0.1%	0.1%	4.8%	100%
2	257.34	22.69	0.43	0.00	19.68	301
	85.7%	7.6%	0.1%	0.0%	6.6%	100%
3	262.15	18.96	0.45	0.00	20.37	302
	86.8%	6.3%	0.1%	0.0%	6.7%	100%
4	444.87	36.90	0.73	0.00	33.29	516
	86.3%	7.2%	0.1%	0.0%	6.5%	100%
5	272.44	44.90	0.43	0.00	19.69	338
	80.7%	13.3%	0.1%	0.0%	5.8%	100%
6	184.92	17.31	0.41	0.00	15.78	219
	84.7%	7.9%	0.2%	0.0%	7.2%	100%
7	184.99	13.38	0.36	0.00	15.88	215
	86.0%	6.4%	0.2%	0.0%	7.4%	100%
8	1945.20	320.30	2.50	1.89	116.60	2386
	81.5%	13.4%	0.1%	0.1%	4.9%	100%

Table 15. Equivalent annual dose rates [mSv per year] in the spacecraft model room with the wall made of 0.5 cm Al and 20 cm CnM

Position (fig. 29)	Proton	Alpha	Photon	Electron	Neutron	Total
1	88.58	8.80	0.09	0.00	3.81	512
	87.5%	8.7%	0.1%	0.0%	3.8%	100%
2	43.06	2.32	0.06	0.00	2.33	242
	90.1%	4.9%	0.1%	0.0%	4.9%	100%
3	43.06	2.32	0.06	0.00	2.33	242
	90.1%	4.9%	0.1%	0.0%	4.9%	100%
4	75.17	4.00	0.10	0.00	4.08	421
	90.2%	4.8%	0.1%	0.0%	4.9%	100%
5	48.88	5.97	0.07	0.00	2.27	289
	85.5%	10.4%	0.1%	0.0%	4.0%	100%
6	29.86	1.88	0.06	0.00	1.75	170
	89.0%	5.6%	0.2%	0.0%	5.2%	100%
7	29.86	1.88	0.06	0.00	1.75	170
	89.0%	5.6%	0.2%	0.0%	5.2%	100%
8	361.10	39.33	0.44	0.27	15.87	2107
	86.6%	9.4%	0.1%	0.1%	3.8%	100%

87~90% to the total dose, alphas contribute around 6%, and the secondary neutrons give additional ~5%. The dose rates due to secondary photons and electrons remain low as in the previous case.

If the overall density thickness is increased, the new shielding should naturally reduce the annual dose rates. The additional model with 0.5 cm Al and 40 cm CnM (giving 39.3 g/cm²) was in-

Table 16. Equivalent annual dose rates [mSv per year] in the spacecraft model room with the wall made of 0.5 cm Al and 40 cm CnM

Position (fig. 29)	Proton	Alpha	Photon	Electron	Neutron	Total
1	255.30	11.12	0.32	0.00	13.47	280
	91.1%	4.0%	0.1%	0.0%	4.8%	100%
2	112.00	4.72	0.18	0.00	7.64	125
	89.9%	3.8%	0.1%	0.0%	6.1%	100%
3	112.00	4.72	0.18	0.00	7.64	125
	89.9%	3.8%	0.1%	0.0%	6.1%	100%
4	199.28	8.40	0.31	0.00	12.66	221
	90.3%	3.8%	0.1%	0.0%	5.7%	100%
5	151.75	8.76	0.22	0.00	8.47	169
	89.7%	5.2%	0.1%	0.0%	5.0%	100%
6	85.22	3.92	0.14	0.00	5.79	95
	98.6%	4.1%	0.1%	0.0%	6.1%	100%
7	58.22	3.92	0.14	0.00	5.79	95
	89.6%	4.1%	0.1%	0.0%	6.1%	100%
8	649.30	35.64	0.98	0.65	34.48	721
	90.0%	4.9%	0.1%	0.1%	4.8%	100%

Table 17. Dose rate [mSv per year] comparison for different combination of shielding materials

Position (fig. 29)	0.5 cm Al + 20 cm PE	0.5 cm Al + 20 cm CnM	0.5 cm Al + 40 cm CnM
1	578	512	280
	100%	89%	55%
2	301	242	125
	100%	80%	52%
3	302	242	125
	100%	80%	52%
4	516	421	221
	100%	82%	52%
5	338	289	169
	100%	86%	58%
6	219	170	95
	100%	78%	56%
7	215	170	95
	100%	79%	56%
8	2386	2107	721
	100%	88%	34%

cluded and the dose values are listed in tab. 16. Protons contribute around 90% to the total dose, alphas contribute 4~5%, and secondary neutrons add 5~6%.

The comparison of the dose rates obtained when using Al/CnM shielding to that using the Al/PE shielding is summarized in tab. 17. It can be seen that the equivalent annual dose rates decrease 11~21% with Al/CnM of the same density thick-

ness, while it is almost 50% lower with 40 cm CnM (corresponding to 39.3 g/cm² density thickness).

CONCLUSION

Radiation is a main concern for long term manned missions to space. It also represents a limiting criterion for the duration and distance of a travel. The radiation in space is represented as a complex radiation mix consisting of high energy ions, protons, alphas, and electrons. With current technology, it does not seem feasible for the entire spacecraft to be shielded against all types of radiation, as that would greatly increase the mass of the ship. What needs to be done is to determine what areas of the ship need to be shielded, taking into account living space, power and propulsion systems, consumables, and repair needs. Lightweight materials must be utilized to keep the overall shield mass low, to attenuate satisfactorily the expected mix of radiation in space and assure the crew protection. Examining the effectiveness of such materials exposed to radiation fields of different intensities and types and having an accurate numerical model to predict the material irradiation is crucial in designing the manned missions to outer space.

The design and evaluation of the required radiation protection for the astronauts traveling to the destinations beyond the Moon are both greatly affected by the number of parameters all being driven by immense degree of uncertainty:

- (a) definition of the space radiation environment important to develop and establish the spacecraft design criteria introduces by far the greatest overall uncertainty in the radiation dose prediction for manned mission to deep space,
- (b) definition of maximum acceptable dose for astronauts,
- (c) manned space craft is large and geometrically a very complex system (no design for a manned mission to deep space has been yet known) in which the biggest uncertainty is introduced by the uncertainty in mass distribution, and
- (d) computational models are accurate as much as the spacecraft design and mass distribution are known; that is why all models are usually simplified and as such used in developing the design areas for the number of parameters that introduce the potential errors in estimates of the maximum dose rates and material performance in assumed radiation field in space.

The adopted criteria (see section on the space radiation design criteria) for the analysis shown in this paper, of keeping the annual dose rate below 200 mSv per year and the shielding density thickness close to 20 g/cm², indicate that the best materials are PE and CnM. Further optimizations are necessary and at this point highly dependent on the spacecraft design. National Academy of Sciences in the USA

has recently established a Committee that has a two year appointment to evaluate the best design for shielding the astronauts against space radiation on their travel to and stay at the Moon, and on the potential travel to Mars.

ACKNOWLEDGEMENTS

The authors would like to thank Randy Hopkins for his time and valuable consultations, and Dr. Luis Zalamea for his information regarding the carbo-nano materials. Research has been partially supported through US Department of Energy "mini-INIE" project grant.

REFERENCES

- [1] ***, NASA Space Vehicle Design, Space Radiation Protection, NASA SP-8054, 1970
- [2] ***, MCNPXTM – User's Manual Version 2.5.0, (Ed. D. B. Pelowitz), LA-CP-05-0369, 2005
- [3] ***, Lawrence Livermore National Lab, COG User Manual, last modified on March 7, 1996, Available from http://www-pat.llnl.gov/N_Div/COG/COG_home.html [cited April 20, 2006]
- [4] ***, NASA Space Vehicle Design Criteria, Space Radiation Protection, NASA SP-8054, 1970
- [5] Adams, Jr. J. H., Hathaway, D. H., Grugel, R. N., Watts, J. W., Parnell, T. A., Gregory, J. C., Winglee, R. M., Revolutionary Concepts of Radiation Shielding for Human Exploration of Space, NASA/TM-2005-213688, NASA, 2005
- [6] ***, NASA Space Vehicle Design Criteria, Nuclear and Space Radiation Effects on Materials, NASA SP-8053, 1970
- [7] Heilbronn, L., Production of Neutrons from Interactions of GCR-Like Particles, NASA Conference Publication 3360, 1997, pp. 247-259
- [8] Thibeault, S. A., Wilson, J. W., Long, Jr. E. R., Kiefer, R. L., Glasgow, M. B., Orwoll, R. A., Shielding Materials Development and Testing Issues, NASA Conference Publication 3360, pp. 397-425, 1997
- [9] Tylka A., J., Dietrich, W. F., Boberg, P. R., Smith, E. C., Adams, J. H., Single Event Upsets Caused by Solar Energetic Heavy Ions, *IEEE Trans. Nucl. Sci.*, Vol. 43 (1996), p. 2758
- [10] Badhwar, G. D., Deep Space Radiation Sources, Models, and Environmental Uncertainty, Shielding Strategies for Human Space Exploration Target, NASA Conference Publication 3360, 1997, pp. 17-28
- [11] Badhwar, G. D., O'Neil, P. M., Galactic Cosmic Radiation Model and Its Application, *Advances in Space Research*, 17 (1996), pp. 7-17
- [12] Townsend, L. W., Implications for the Space Radiation Environment for Human Exploration in Deep Space, *Radiation Protection Dosimetry*, 115 (2005), 1-4, doi:10.1093/rpd/ncil141. pp. 44-50
- [13] Cucinotta, F. A., Calculations of Cosmic-Ray Helium Transport in Shielding Materials, NASA Technical Paper 3354, 1993

- [14] Cucinotta, F. A., Wilson J. W., Assessment of Current Shielding Issues, NASA Conference Publication 3360, 1997, pp. 448-467
- [15] Wilson, J. W., Miller, J., Konradi, A., Cucinotta, F. A., Shielding Strategies for Human Space Exploration, NASA Conference Publication 3360
- [16] Reitz, G., Facius, R., Sandler, H., Radiation Protection in Space, *Acta Astronautica*, 35 (1995), 45, pp. 313-338
- [17] ***, Radiation Shielding Solutions for Manned Mission to Mars, Technical Report, PU/NE 05-05, Purdue University, West Lafayette, IN, USA, 2005
- [18] Dale, C. J., Marshall, P. W., Summers, G. P., Wolicki, E. A., Displacement Damage Equivalent to Dose, *Appl. Phys. Lett.*, 54 (1989), pp. 451-453
- [19] ***, National Institute of Standards and Technology Standard Reference Database 124, 2006, Physics Laboratory, available from <http://physics.nist.gov/PhysRefData/Star/Text/PSTAR.html> [cited April 24 2006]
- [20] Heng, H-M., Yang, Q-H., Chang, L., Hydrogen Storage in Carbon Nanotubes, *Carbon*, 39 (2001), pp. 1447-1454

**Мануел ШТЕЈНБЕРГ, Шанђие ШИАО, Надар САТВАТ,
Фелиса ЛИМОН, Џон ХОПКИНС, Татјана ЈЕВРЕМОВИЋ**

**АНАЛИЗА ЗАШТИТЕ ОД ЗРАЧЕЊА АСТРОНАУТА НА ПУТУ ДО МАРСА
– Критеријуми, прегледна студија и прелиминарни модел –**

Потенцијални лет са астронаутима изван Земљине орбите је ограничен временском компонентном путовања као и аспектима заштите од космичког зрачења. Данашња технологија свемирских ракета је базирана на погону који користи хемијско гориво. Те врсте машина немају могућност да обаве дуге летове као што је пут до Марса са посадом због огромне количине течног горива потребног за тако дуга свемирска путовања. Специфична енергија ослобођена у нуклеарном гориву је милион пута већа од исте добијене из хемијског горива; стога је потпуно јасно да је нуклеарно гориво једина опција која би омогућила дуг пут у свемир. С друге стране, потенцијална мисија која би укључила транспорт људи и њихов нешто дужи боравак на Месецу би захтевала стабилно и сигурно решење за производњу енергије на Месецу (на почетку 21. века не постоји ни једно друго решење осим нуклеарне енергије које би омогућило сигурно и дуготрајно снабдевање неопходном струјом и топлотом). НАСА сматра да је маса и тежина материјала неопходног за заштиту од зрачења током дугог пута до Марса други најважнији ограничавајући аспект мисије. НАСА је 2006. године идентификовала потребу да се евалуира и анализира потенцијална веза у познавању и разумевању нивоа и типова зрачења од значаја за астронауте током пута до Марса. НАСА је с тога започела свеобухватну студију која би требало за две године да произведе задовољавајући дизајн заштите од космичког зрачења који би био саставни део свемирске летелице и задовољавао критеријуме дозвољених нивоа зрачења. Да би се смањила свеукупна маса летелице НАСА је фокусирана на истраживања која би довела до нових материјала (композиата) са више намена и више функција, а који би истовремено представљали задовољавајућу заштиту од космичког зрачења.

Лабораторија за прорачуне транспорта неутрона и моделовање геометрија (НЕГЕ) у школи за нуклеарни инжењеринг на Пурдју Универзитету коју води професор Татјана Јевремовић, започела је 2004. године евалуацију различитих лаких материјала за употребу у свемирским летелицама ка Марсу. Прелиминарни резултати прегледне студије приказани су у овом раду.

Кључне речи: дуга путовања у свемир, космичко зрачење, заштита од зрачења, Метода Карло мейода, транспорт зрачења